

†

Nonuniversality of the interference quantum correction to conductivity beyond the diffusion regime

A. V. Germanenko,¹ G. M. Minkov,² A. A. Sherstobitov,² and O. E. Rut¹

*¹Institute of Physics and Applied Mathematics,
Ural State University, 620083 Ekaterinburg, Russia*

²Institute of Metal Physics RAS, 620219 Ekaterinburg, Russia

(Dated: February 6, 2008)

Abstract

Results of numerical simulation of the weak localization in two-dimensional systems in wide range of magnetic field are presented. Three cases are analyzed: (i) the isotropic scattering and randomly distributed scatterers; (ii) the anisotropic scattering and randomly distributed scatterers; (iii) the isotropic scattering and the correlated distribution of the scatterers. It is shown that the behavior of the conductivity beyond the diffusion regime strongly depends on the scattering anisotropy and correlation in the scatterer distribution.

PACS numbers: 73.20.Fz, 73.61.Ey

Interference (or weak localization) quantum correction to the conductivity arises from interference of electron waves scattered along closed trajectories in opposite directions. An external magnetic field applied perpendicular to the two-dimensional (2D) layer destroys the interference and suppresses the quantum correction. It results in anomalous negative magnetoresistance, which is experimentally observed in many disordered 2D systems.¹ Theoretically, this problem was studied only for the case of random distribution of scattering centers and isotropic scattering (comparative analysis of different calculation approaches has been done in Ref. 2). As a rule, these conditions are not fulfilled in real semiconductor structures. First of all, the scattering by ionized impurities dominates often in semiconductors at low temperatures. This scattering is strongly anisotropic, in particular, in heterostructure with remote doping layers. Besides, the impurity distribution is correlated to some extent due to Coulomb repulsion of the impurity ions at the temperatures of crystal growth.

In the present work the role of scattering anisotropy in the quantum correction to the conductivity is investigated through a computer simulation. It is shown that the interference quantum correction is nonuniversal beyond the diffusion regime, when it is determined by a short closed paths with relatively small number of collisions. Its behavior with temperature and magnetic field change depends on the scattering details strongly.

The weak-localization phenomenon can be described in the framework of quasiclassical approximation which is justified under the condition $k_F l \gg 1$, where k_F is the Fermi wave vector, l is the mean free path. In this case the conductivity correction is expressed through the classical *quasi*probability density W for an electron to return to the area of the order $\lambda_F l$ around the start point^{3,4,5,6}

$$\delta\sigma = -\sigma_0 \frac{\lambda_F l}{\pi} W = -2\pi l^2 G_0 W, \quad (1)$$

where $G_0 = e^2/(2\pi^2\hbar)$, $\lambda_F = 2\pi/k_F$, and $\sigma_0 = \pi G_0 k_F l$ is the Drude conductivity. Prefix *quasi*- means that W takes into account the dephasing of interfering waves caused by external magnetic field and inelastic processes. Expression (1) allows ones to calculate the conductivity correction at any magnetic field and temperature.⁷ To find W and l , we simulate the motion of a particle over the 2D plane with scattering centers in it. This technique was described in details in our paper, Ref. 8. Here is outline only. The plane is represented as a lattice. The scatterers with a given cross-section are placed in a part of lattice sites with the use of a random number generator. A particle is launched from some random point,

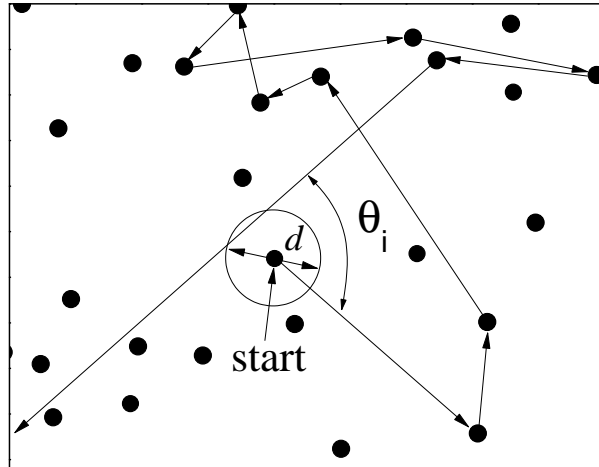


FIG. 1: Sketch of model 2D system and fragment of the i -th closed path near starting point.

then it moves with a constant velocity along straight lines, which happen to be terminated by collisions with the scatterers. After collision it changes the motion direction. If the particle passes near the starting point at the distance less than $d/2$ (where d is a prescribed value, which is small enough), the path is perceived as being closed. Its length and enclosed algebraic area are calculated and kept in memory. The particle walks over the plane until it escapes the lattice. As this happens one believes that the particle has left to infinity and will not return. A new start point is chosen and all is repeated. A fragment of one of the closed paths near the starting point is shown in Fig. 1.

The simulation has been carried out for three systems. In system A the scatterers are distributed randomly, the scattering is isotropic that physically corresponds to a short-range scattering potential. In the system B the scatterers are distributed randomly and scattering is anisotropic. The angle dependence of scattering probability for this case is presented in the inset in Fig. 2(b). It is close to that for the heterostructure with δ doped barrier in which impurities are spaced from the 2D gas. The anisotropy shown can correspond, for instance, to a semiconductor heterostructure with impurity density of about 10^{12} cm^{-2} and a spacer thickness of 50 \AA . Finally, the system C is characterized by isotropic scattering, but the distribution of scatterers is quite correlated. Namely, the nearest neighbor distance is not less than 20 whereas the mean distance between scatterers was about 30 (hereafter length and area are measured in units of lattice parameter and its square, respectively).

The parameters used in simulation are the following: $d = 5$; the number of launches

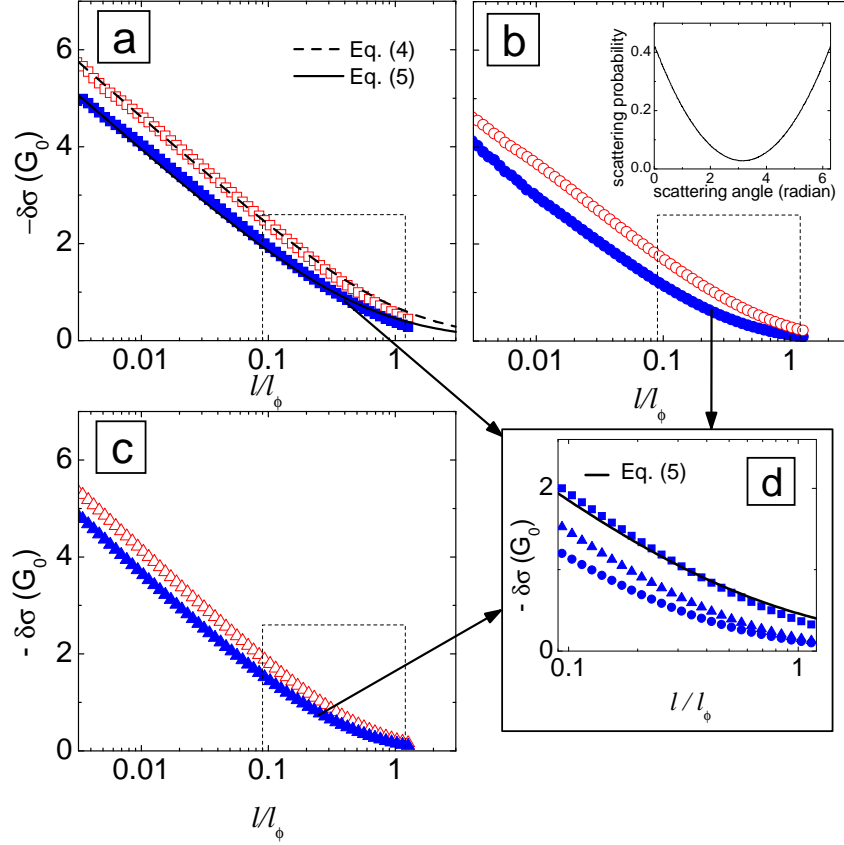


FIG. 2: The interference quantum correction in zero magnetic field as a function of l/l_ϕ . (a) – Scattering is isotropic, the distribution of scatterers is random (system A). Dashed and solid lines are the analytical results, Eq. (4) and Eq. (5), respectively. (b) – Scattering is anisotropic with the angle dependence of the scattering probability shown in the inset, the distribution of scatterers is random (system B). (c) – Scattering is isotropic, the distribution of scatterers is correlated (system C). (d) – The same data are presented in enlarged scale. Open and solid symbols correspond to Eqs. (2) and (3), respectively.

$10^5..10^6$; the dimensions of the lattice is $10^4 \times 10^4$. The cross-section of the scatterers is equal to 7. The density of scatterers is such that the transport mean-free path is about 120 for all three systems. For illustration, let us set the lattice parameter equal to 5 \AA . Then our model provides an example of 2D system in which the transport mean-free path is $l = 600 \text{ \AA}$ and $B_{tr} \simeq 0.09 \text{ T}$.

As shown in Ref. 8, the value of $\delta\sigma$ for the model systems can be calculated as follows

$$\frac{\delta\sigma(b)}{G_0} = -\frac{2\pi l}{d \cdot N} \sum_i \cos\left(\frac{bS_i}{l^2}\right) \exp\left(-\frac{l_i}{l_\phi}\right), \quad (2)$$

where summation runs over all closed trajectories among a total number of trajectories N , $b = B/B_{tr}$ is the magnetic field measured in units of transport magnetic fields $B_{tr} = \hbar/(2el^2)$, S_i and l_i stand for the algebraic area and length of the i -th trajectory, respectively, l_ϕ is the phase breaking length connected in reality with the phase relaxation time τ_ϕ through the Fermi velocity v_F , $l_\phi = v_F\tau_\phi$ (not to be confused with the diffusion phase breaking length $L_\phi = \sqrt{D\tau_\phi}$, where D is the diffusion coefficient). Equation (2) takes into account only the coherent backscattering correction to the conductivity. In order to take into account the nonbackscattering processes, which are important in the ballistic regime,⁶ each term in Eq. (2) should be multiplied by the factor $[1 - \cos(\theta_i)]$,⁸ where θ_i is the angle between the first and last segments of the i -th closed path (see Fig. 1):

$$\frac{\delta\sigma(b)}{G_0} = -\frac{2\pi l}{d \cdot N} \sum_i [\dots] [1 - \cos(\theta_i)]. \quad (3)$$

In what follows the results obtained from both Eq. (2) and Eq. (3) will be considered.

In Fig. 2, the results of our simulation for $\delta\sigma(b = 0)$ are plotted against the ratio l/l_ϕ (or that is just the same against τ/τ_ϕ). Open symbols correspond to the case when only the backscattering processes are taken into account, i.e., $\delta\sigma$ is calculated from Eq. (2). Data presented by solid symbols are obtained from Eq. (3) and, thus, include both back- and nonbackscattering contributions. In the assumption of $\tau_\phi \propto T^{-p}$, where $p > 0$, this figure illustrates the temperature dependence of the interference quantum correction to the conductivity. The upper solid line in Fig. 2(a) shows the known theoretical results for the backscattering contributions in weak localization^{4,6}

$$\frac{\delta\sigma}{G_0} = -\ln\left(1 + \frac{\tau_\phi}{\tau}\right). \quad (4)$$

The lower line is the results of Ref. 6 where both the backscattering and nonbackscattering contributions are taken into account

$$\begin{aligned} \frac{\delta\sigma}{G_0} &= -\ln\left(1 + \frac{\tau_\phi}{\tau}\right) \\ &+ \frac{1}{1 + 2\tau_\phi/\tau} \ln\left(1 + \frac{\tau_\phi}{\tau}\right) + \frac{\ln 2}{1 + \tau/2\tau_\phi}, \end{aligned} \quad (5)$$

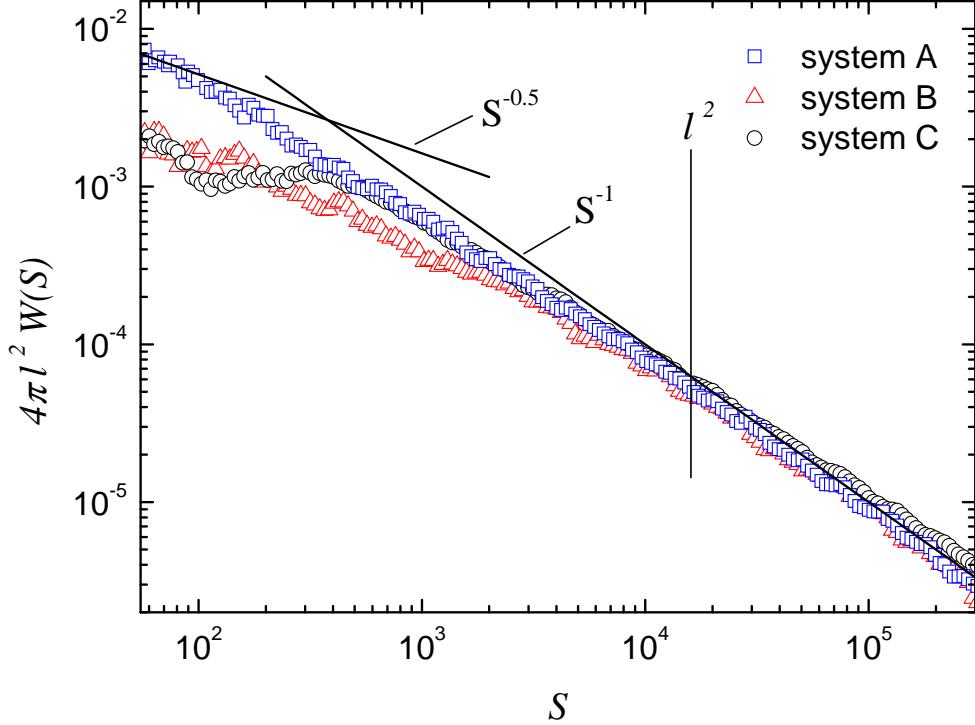


FIG. 3: The area distribution function of closed paths, obtained from the simulation procedure. Solid lines are the asymptotes for the purely ballistic and diffusive motion. Since $W(S)$ is identical for $S > 0$ and $S < 0$, only the range of positive algebraic area is shown.

As is clearly seen the simulation and the theoretical data are almost the same. Thus, one can believe that the simulation procedure does not fail and for $l/l_\phi > 3 \times 10^{-3}$ our model system is equivalent to an unbounded 2D system and the simulation gives correct results.

Inspection of Fig. 2 shows that the temperature dependence of $\delta\sigma$ in the systems with the anisotropic scattering (system B) and with the correlation (system C) is very close to that for the system with isotropic scattering and random distribution of scatterers (system A). In all three cases the temperature dependence of $\delta\sigma$ is close to the logarithmic one for low l/l_ϕ values, i.e., for low temperatures in real systems. The only difference is the absolute value of the interference correction for a fixed l/l_ϕ value. The relative difference in the temperature behavior for different systems becomes more pronounced at $l/l_\phi \gtrsim 0.1$ [see Fig. 2(d)] when the quantum correction is mainly determined by the closed paths with a small number of collisions (so called ballistic regime). Thus, already analysis of the data carried out in the absence of magnetic field shows that the interaction correction feels the details of scattering.

Before to discuss the magnetoconductivity let us consider the area distribution function of closed paths $W(S)$ because namely it determines the magnetic field dependence of the interference induced magnetoresistance.⁸ As is seen from Fig. 3, the dependence $4\pi l^2 W(S)$ mostly follows S^{-1} -law for all three systems while $S > l^2$. This is in agreement with the result of the diffusion theory for infinite 2D system which gives $4\pi l^2 W(S) = S^{-1} \tanh(\pi S/l^2) \simeq S^{-1}$ for $S > l^2$.^{8,9} Thus, despite the fact that the distribution of scatterers is correlated in the system C, this system shows the diffusive behavior for large number of scattering events. A significant difference in $W(S)$ is evident for small areas enclosed, $S \ll l^2$, where the main contribution to $W(S)$ comes from the closed paths with small number of collisions. It is obvious that details of single scattering event and the distribution of scatterers are important for statistics of short closed paths. For system A the area distribution function $W(S)$ tends to the asymptotic $S^{-1/2}$ law valid when $S \ll l^2$ [see Refs. 5 and 10]. For other two systems, $W(S)$ demonstrate more complicated behavior in our S -range.

So, this qualitative consideration shows that the low-field magnetoresistance ($b \ll 1$) which is mainly determined by the paths with large areas enclosed ($S \gg l^2$) must be similar for all three systems. Strong difference should appear only in high magnetic field ($b \gg 1$) when short closed paths with $S \ll l^2$ are suspended from the interference.

Now we are in position to discuss the magnetoconductance $\Delta\sigma(b) = \sigma(b) - \sigma(0)$. Namely this quantity is usually measured to obtain the phase relaxation time experimentally. For this purpose an experimental $\Delta\sigma$ -vs- b plot are fitted to the one of the known theoretical expressions with τ_ϕ as fitting parameter. The formula¹¹ is widely used for this purpose

$$\Delta\sigma(b) = \alpha G_0 \left\{ \psi \left(\frac{1}{2} + \frac{\gamma}{b} \right) - \psi \left(\frac{1}{2} + \frac{1}{b} \right) - \ln \gamma \right\}, \quad (6)$$

where $\gamma = \tau/\tau_\phi$, $\psi(x)$ is a digamma function, α is the prefactor. Theoretically, the prefactor is equal to unity. Experimentalist uses it as the fitting parameters together with τ_ϕ (or γ). Below we follow this way considering our simulation data as the experimental ones. Then, we compare the fitting value of γ with τ/τ_ϕ used in the simulation procedure.

Fig. 4(a) shows the low-field ($b < 0.2$) magnetoconductance $\Delta\sigma(b)$ calculated from Eq. (2) for different τ_ϕ/τ values. As expected all systems demonstrate close behavior. It has been also found that taking into account nonbackscattering processes does not practically change the magnetic field dependence of $\Delta\sigma(b)$ for all the systems (insensitivity of low-field magne-

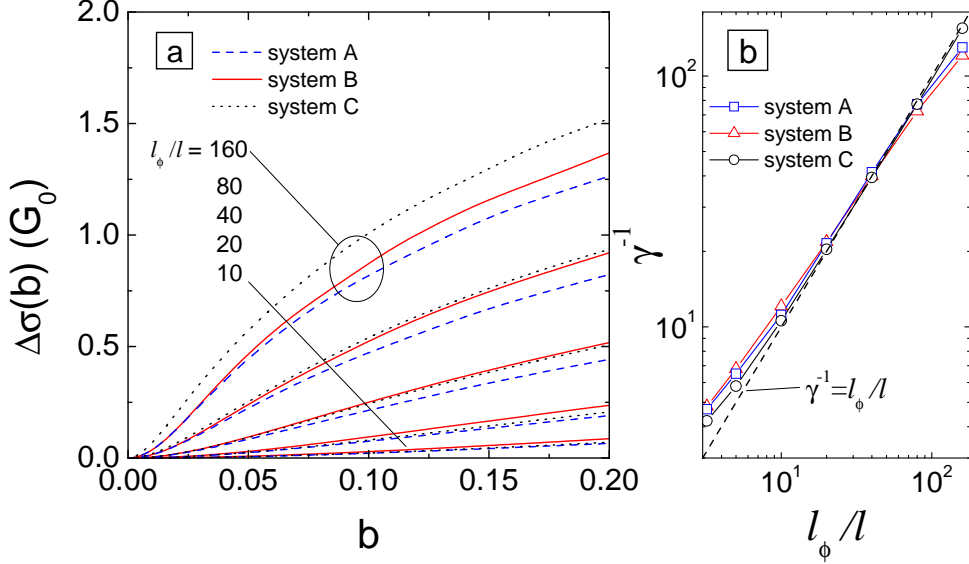


FIG. 4: The low-field dependence of $\Delta\sigma$ for different l_ϕ/l values (a) and the results of data processing of this curves with the help of Eq. (6) (b).

toconductance to the nonbackscattering processes is discussed in Refs. 6 and 8).

If one considers the simulated $\Delta\sigma$ -vs- b data shown in Fig. 4(a) as experimental ones and fits them by Eq. (6) as described above we obtain a nice coincidence in all the cases. How the fitting value of γ matches the value of $l/l_\phi = \tau/\tau_\phi$ put in Eq. (2) is shown in Fig. 4(b). As seen the fitting procedure gives the value of γ which can differ by a factor of about two from the value of l/l_ϕ . This may be explained by the fact that Eq. (6) is derived within the framework of the diffusion approximation ($\gamma \ll 1$, $b \ll 1$), which is too strong.^{4,7,8}

Figure 5 shows the dependencies of $\delta\sigma(b)$, calculated for different τ/τ_ϕ values with the help of Eqs. (2) and (3) in wider range of magnetic field including the ballistic regime $b \gg 1$. It is seen that the behavior of $\delta\sigma(b)$ for $b > 1$ strongly depends on scattering details for both types of calculations. It is evident much better when considering the $\Delta\sigma$ -vs- b data (Fig. 6). So the magnetic field dependences of $\delta\sigma$ and $\Delta\sigma$ are saturated in lower magnetic field when the scattering is anisotropic or distribution of scatterers is correlated. Such peculiarities directly follow from the difference in the area distribution functions at $S < l^2$ (see Fig. 3). There is a appreciable deficit of the paths with small area enclosed, $S \lesssim 200$, in systems B and C as compared with system A.

In conclusion, the magnetic filed behavior of the low-filed magnetoconductance in two-dimensional systems due to suppression of the quantum interference is not universal beyond

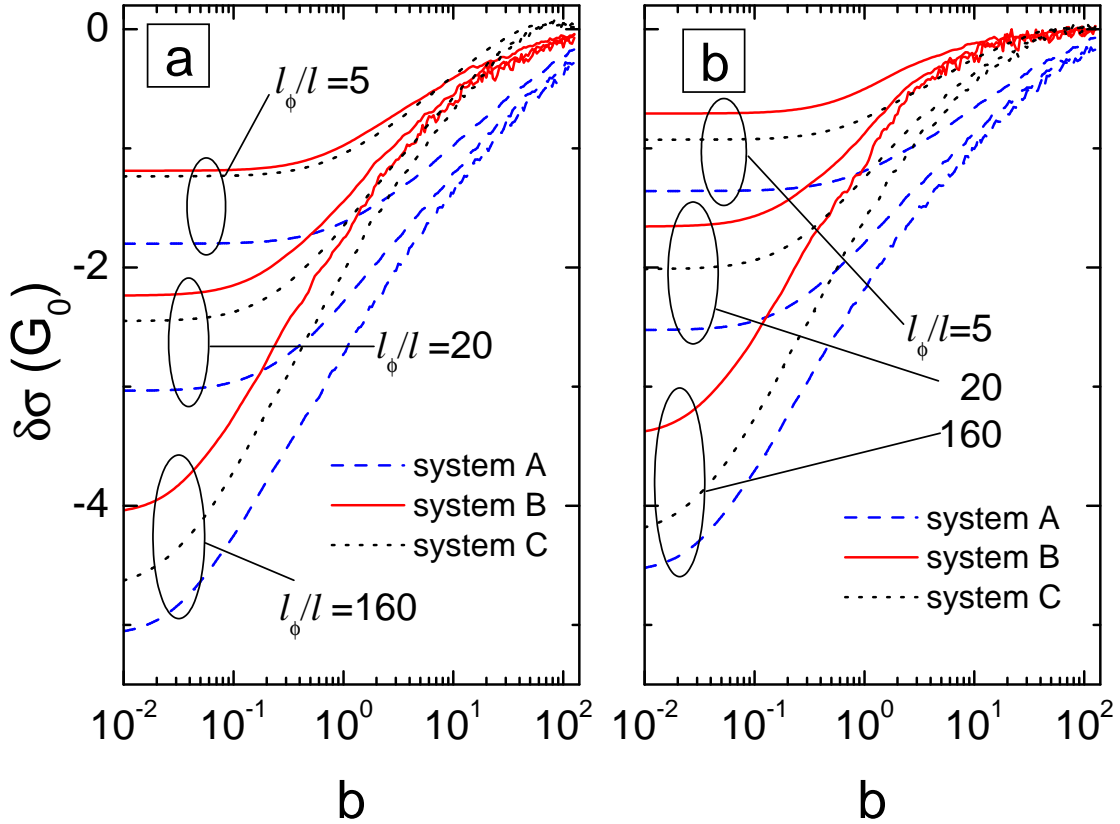


FIG. 5: The magnetic field dependence of $\delta\sigma$ for different l_ϕ/l values, obtained with the help Eq. (2) (a) and Eq. (3) (b).

the diffusion regime ($b \gg 1$ or $\tau/\tau_\phi \sim 1$). It strongly depends on the scattering details. The use of theoretical expressions which were derived for the 2D systems with isotropic scattering and the random distribution of the scatterers for interpretation of the experimental data beyond the diffusion regime, that is a typical situation for experiments on high-mobility 2D heterostructures, can give inadequate information on the value and temperature dependence of the phase relaxation time.

We would like to thank Igor Gornyi for a number of illuminating discussions. This work was supported in part by the RFBR (Grants 04-02-16626, 05-02-16413, and 06-02-16292), the CRDF (Grants EK-005-X1 and Y1-P-05-11), and by the Grand of President of Russian

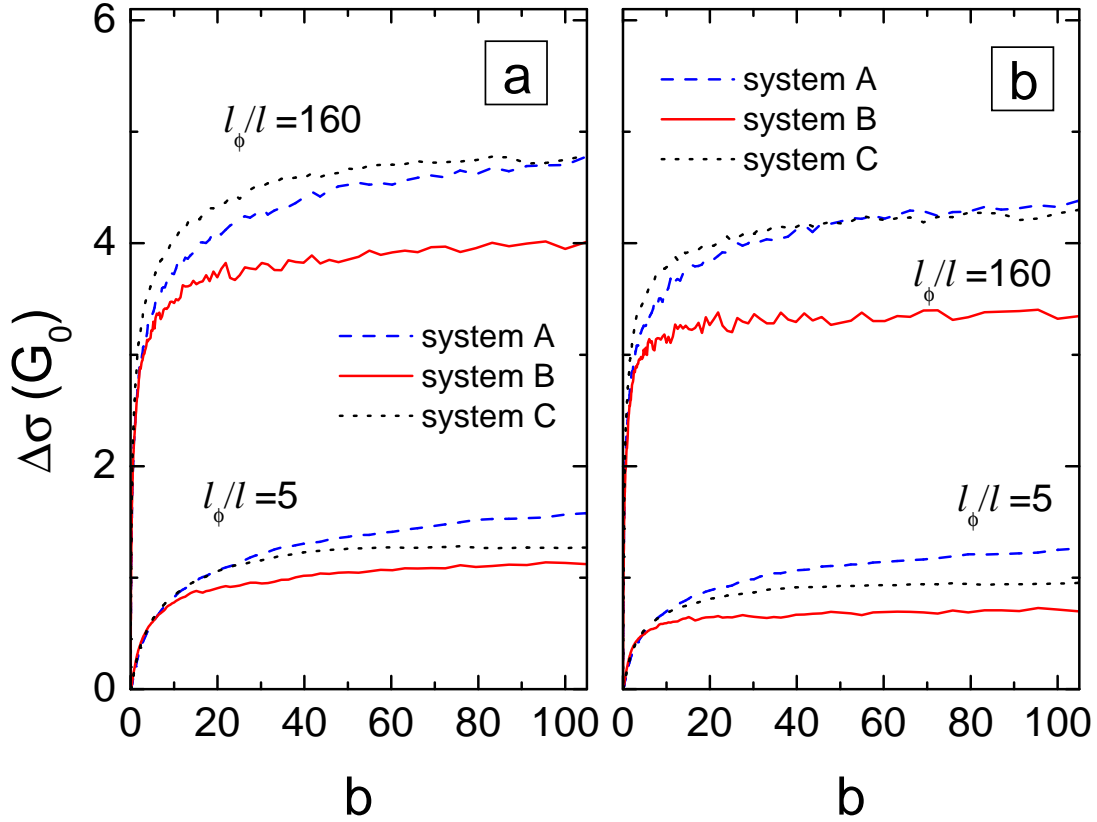


FIG. 6: The magnetic field dependence of $\Delta\sigma = \delta\sigma(b) - \delta\sigma(0)$ for different l_ϕ/l values, obtained using Eq. (2) (a) and Eq. (3) (b).

Federation for young scientists MK-1778.2205.2.

-
- ¹ B. L. Altshuler and A. G. Aronov, in *Electron-Electron Interaction in Disordered Systems*, Edited by A. L. Efros and M. Pollak (North Holland, Amsterdam, 1985).
- ² S. McPhail, C. E. Yasin, A. R. Hamilton, M. Y. Simmons, E. H. Linfield, M. Pepper, and D. A. Ritchie, *Phys. Rev. B* **70**, 245311 (2004).
- ³ L. P. Gorkov, A. I. Larkin, and D. E. Khmel'nitskii, *Pisma Zh. Eksp. Teor. Fiz.* **30**, 248 (1979) [*JETP Lett* **30**, 248 (1979)].
- ⁴ S. Chakravarty and A. Schmid, *Phys. Rep.* **140**, 193 (1986).
- ⁵ M. I. Dyakonov, *Solid State Commun.* **92**, 711 (1994).
- ⁶ A. P. Dmitriev, V. Yu. Kachorovskii, and I. V. Gornyi, *Phys. Rev. B* **56**, 9910 (1997).

- ⁷ H. P. Wittman and A. Schmid, *J. Low. Temp. Phys.* **69**, 131 (1987).
- ⁸ G. M. Minkov, A. V. Germanenko, V. A. Larionova, S. A. Negashev, and I. V. Gornyi, *Phys. Rev. B* **61**, 13164 (2000).
- ⁹ K. V. Samokhin, *Phys. Rev. E* **59**, R2501 (1999).
- ¹⁰ A. Zduniak, M. I. Dyakonov, and W. Knap, *Phys. Rev. B* **56**, 1996 (1997).
- ¹¹ S. Hikami, A. Larkin, and Y. Nagaoka, *Prog. Theor. Phys.* **63**, 707 (1980).